Available online at www.sciencedirect.com

ScienceDirect

Energy Procedia 92 (2016) 109 – 115

Energy Procedia

6th International Conference on Silicon Photovoltaics, SiliconPV 2016

Simulation-based efficiency gain analysis of 21.2%-efficient screen-printed PERC solar cells

Christopher Kranz[a,*], Jan H. Petermann[a], Thorsten Dullweber[a], Rolf Brendel[a,b]

[a]*Institute for Solar Energy Research Hamelin (ISFH), Am Ohrberg 1, D-31860 Emmerthal, Germany*
[b]*Department of Solar Energy, Institute of Solid-State Physics, Leibniz Universität Hannover, Appelstr. 2, D-30167 Hanover, Germany*

Abstract

Passivated Emitter and Rear Cells (PERC) with efficiencies well above 20% are likely to become the next mass production technology. A quantification of all power loss mechanisms of such industrial PERC cells is helpful in prioritizing future efficiency improvement measures. We report on a numerical simulation of the power losses of a 21.2 %-efficient industrial PERC cell using extensive experimental input data. Our synergetic efficiency gain analysis relies on deactivating single power loss mechanisms in the simulation at a time to access the full potential power gain related to that mechanism. The complete analysis therefore explains the efficiency gap between the industrial PERC solar cell and the theoretical maximum efficiency of a crystalline Si solar cell. Based on the simulations, the largest single loss mechanism is front grid shadowing followed by recombination in the emitter and its surface. All individual resistive losses, all individual optical losses and all (avoidable) individual recombination losses sum up to efficiency gains of 0.8%, 1.6%, and 1.3 %, respectively, which is 3.7% in total. The efficiency gap between real and ideal solar cell is, however, much larger with 7.3%. The discrepancy is mainly due to the non-linear behaviour of recombination-based power losses which adds synergetic efficiency enhancements.

Peer review by the scientific conference committee of SiliconPV 2016 under responsibility of PSE AG.

Keywords: PERC solar cells; screen-printing; device simulation; power loss analysis

* Corresponding author. Tel.: +49(0)5151-999 643; fax: +49(0)5151-999 400.
E-mail address: kranz@isfh.de

Peer review by the scientific conference committee of SiliconPV 2016 under responsibility of PSE AG.
doi:10.1016/j.egypro.2016.07.038

1. Introduction

As the best industrial-type Passivated Emitter and Rear Cells (PERC) achieve efficiencies of 21% and beyond [1,2,3], a quantification of the impact of all power loss mechanisms is required to ensure that future technological improvements reduce the dominating losses and hence provide a high efficiency improvement. The Free Energy Loss Analysis (FELA) [4] frequently used in solar cell analysis accounts for electrical power losses and represents those as free energy dissipation rates. Therefore the total extracted power P of a solar cell is the free energy generation rate $\dot{F}_g$ minus the free energy dissipation rates caused by recombination $\dot{F}_r$, and transport of charge carriers $\dot{F}_t$:

$$P = \dot{F}_g - \dot{F}_r - \dot{F}_t.$$

For a given working point of a solar cell, one is now able to calculate for example the power loss $\dot{F}_r$ for a specific recombination channel. However, the potential in power gain by improving that recombination channel is higher than $\dot{F}_r$ since avoiding this loss will simultaneously increase the generated free energy

$$\dot{F}_g = \int_V dV\ (E_{FC} - E_{FV})g$$

where g is the generation rate in the cell volume V and $E_{FC} - E_{FV}$ denotes the splitting of the quasi-Fermi level of electrons and holes. The increase of free energy generation is noted by the experimentalist primarily as an increase of the solar cell's open circuit voltage V_{oc} and thus also by change of the working point V_{mpp}. Another approach to power loss analysis [5] uses analytic expressions to calculate the current losses by recombination and imperfect optics. In order to acquire the power losses these current losses are multiplied with the internal voltage of the solar cell at the maximum power point (mpp). This approach, as well as the FELA, does not account for the shift of the working point that goes along with avoiding a loss. Correspondingly the calculated power losses underestimate the potential in power gain and will not add up to the theoretical limit of around 29%. To access the full potential power gains ΔP of each power loss mechanism, we apply the synergetic efficiency gain analysis (SEGA) [6] to our 21.2%-efficient industrial PERC solar cell [2]. The SEGA explains the efficiency gap between the cell under investigation and an ideal cell. It treats optical, electrical and resistive losses on an equal footing and makes these different losses directly comparable.

This paper was presented at the SiliconPV 2015 conference in Constance and is now published within the SiliconPV 2016 proceedings.

2. Numerical model

We model our 21.2%-efficient dual-printed 5 busbar (5BB) PERC solar cell (labeled "group 3" in Ref. 2) which is schematically shown in Fig. 1a) by a 3-step simulation sequence. Raytracing of a textured solar cell with SUNRAYS [7] generates a 1-dimensional photogeneration profile. This profile is then used in a 2D Sentaurus device [8] simulation of a PERC solar cell with a non-textured planar front surface. The unit cell is sketched in Fig. 1b). Finally, the I-V curve resulting from the Sentaurus simulation is used for a grid simulation with LTSpice IV [9] to include resistive losses of front fingers and busbars. All simulations apply realistic input parameters that are either measured on test structures or are taken from the literature.

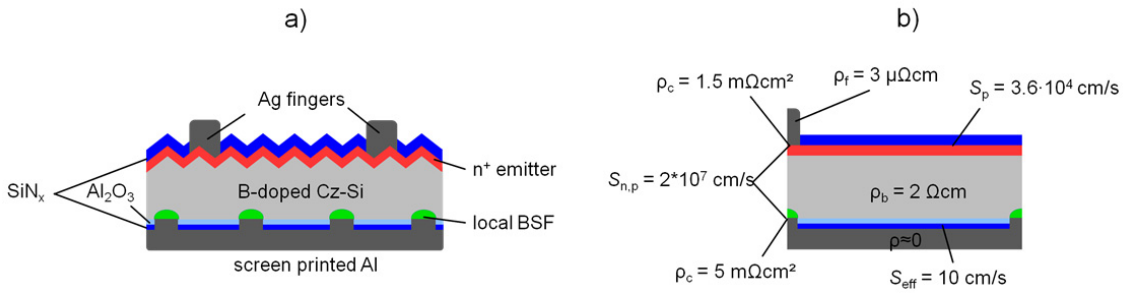

Fig. 1. Schematic drawing of: a) the experimental 21.2% efficient PERC solar cell; b) the unit cell used in Sentaurus Device to simulate the PERC solar cell.

The raytracing simulation applies a SiN_x-coated random pyramid structure and a rear side with a SiN_x layer and an additional Al-layer on it. SUNRAYS provides a Monte-Carlo approach to optical simulation and generates single rays which are traced through the defined geometry. The Sentaurus simulation requires the width of the local Al-contacts that we determine from scanning electron microscope (SEM) images. We simulate the rear side Al contact pitch to be half of the front side pitch in order to keep the simulation domain at a manageable size. Since the experimental ratio of front and rear side pitch is not an integer, we scale the width of the rear contacts to match the actual metallization fraction. All contacts are assumed to be planar. The surface recombination velocity (SRV) of the SiN_x-passivated front surface S_p is adjusted to $3.6 \cdot 10^4$ cm/s in a separate J_0 simulation that uses the measured phosphorus doping profile to match the measured J_{0e} values of 100 fA/cm² of the emitter of our PERC cells [10]. Similarly, the SRV S_n of the local rear contact is adjusted in a simulation with a secondary ion mass spectroscopy (SIMS)-measured local aluminium doping profile to match an effective SRV S_{eff} of about 300 cm/s [11]. For this case however, we find agreement for $S_n = 2 \cdot 10^7$ cm/s [12]. For the recombination at the Al_2O_3/SiN_x rear side passivation we use the parameterization by Black et al. [13] and adjust the interface defect density to a value that results in a recombination current that corresponds a surface recombination velocity of S_{eff} = 10 cm/s, which is a typical value for our Al_2O_3/SiN_x passivation after firing [11]. The bulk material for the solar cell is the one labeled as "Cz 2 Ωcm" in Ref. 14. Annealing under illumination permanently deactivates the BO_x-defects and results in effective lifetimes of around 1 ms at an injection level of $\Delta n = 10^{15}$ cm^{-3}. The photoconductance measurement of the effective lifetime is fitted using 2 Shockley-Read-Hall (SRH) defects at mid-bandgap and the resulting τ_n and τ_p values of both defects are used in the Sentaurus simulation. The contact resistivity of the front Ag finger to the silicon is set to 1.5 mΩcm² as measured by the transmission line method (TLM), whereas the contact resistivity of the aluminum-silicon interface is 5 mΩcm² [15]. A histogram for the distribution of the Ag finger cross sections is obtained by optical profilometer measurements. Using a specific resistivity of 3 µΩcm, based on the finger cross section distribution we calculate the distribution of the local finger line resistances and apply these values to the SPICE simulation in order to account for resistive losses due to non-ideal finger geometries. The resulting effective values of the finger line resistance correspond well to electrical measurements of the finger line resistance. Column 2 of Table 1 summarizes the input parameters applied for the simulation. The simulated PERC cell matches the experimental I-V parameters reasonably well as shown in Table 2.

Table 1. Input parameters of the numerical simulations of the 21.2% efficient PERC solar cell in comparison to the theoretically ideal parameters. (* = measured; # = adjusted to match measured data)

	Realistic input parameters of 21.2% PERC cell	Ideal input parameters
Finger & busbar line resistance	ρ_{finger}= 3 μΩcm*, ρ_{busbar}= 3 μΩcm*	ρ_{finger} and $\rho_{busbar} \approx 0$
Front contact resistance	ρ_c = 1.5 mΩcm²*	$\rho_c \approx 0$ Ωcm²
Bulk & emitter sheet resistance	ρ_b = 2 Ωcm[14], $\rho_{sh} \approx 70$ Ω/sq.[2]	$\rho_b \approx 0$, $\rho_{sh} \approx 0$ Ω/sq.
Rear contact resistance	ρ_c = 5 mΩcm²[15]	$\rho_c \approx 0$ Ωcm²
SiN_x front surface reflection	raytraced random pyramid SiN_x	transmission T=1
Rear surface reflection	raytraced SiN_x/Al layers	R_b=1, Λ = 1
Front grid shadowing	shadowing = 4%[2]	shadowing = 0%
Ag contacts	$S_p = 2 \cdot 10^7$ cm/s[12]	S_p = 1 cm/s
Phosphorus emitter + SiN_x passivation	measured ECV dopant profile, S_p = 36000 cm/s#	τ_{SRH} = 1 s, no Auger, S_p = 1 cm/s
Silicon bulk	SRH model	τ_{SRH} = 1 s
Rear Al-contact + Al-BSF	metal surface: $S_n = 2 \cdot 10^7$ cm/s[12] Al-BSF measured by SIMS	metal surface S_n = 1 cm/s, BSF: τ_{SRH} = 1 s, no Auger
AlO_x/SiN_y rear passivation	S_{eff} = 10 cm/s[11]	$S_{eff} \approx 0$

Table 2. I-V parameters of the experimental 5BB PERC solar cell and the simulated PERC cell. (* = independently confirmed by Fraunhofer ISE Callab)

	η [%]	V_{oc} [mV]	J_{sc} [mA/cm²]	*FF* [%]
Experimental 5BB PERC solar cell [2]	21.22*	662.1	39.8	80.6
Numerical simulation of 5BB PERC cell	21.27	661.5	39.7	80.9

3. Synergetic power gain analysis (SEGA)

We now set each of the input parameters to a theoretically ideal or close to ideal value. This leads to an increase in efficiency. The difference to the initial efficiency quantifies the maximum efficiency gain by every single loss channel. All efficiency gains Δη in this paper are given in %abs, however, to improve readability we use % as an abbreviation. Column 3 of table 1 lists the ideal values of the simulation parameters. The improvements in efficiency Δη for each loss mechanism as resulting from our SEGA are shown in Figure 2. It shows that there is no single large dominating loss in our PERC cell. Only two loss mechanisms have a potential for an efficiency increase by more than 0.5%: This is front grid shadowing (0.82%) and recombination in the emitter and its surface (0.72%). Without surprise the first result agrees well to the quick linear approximation, that avoidance of the 4% front grid shadowing increases the short circuit current J_{SC} by 4% and therefore the efficiency by 4% · 21.2% = 0.82%. The total saturation current density J_0 of our PERC solar cell is around (250 ± 30) fA/cm² as determined by a fit to the IV curve. Thus the emitter with its J_{0e} of 100 fA/cm² has also been expected to dominate recombination losses and to imply a large potential for power gains. The next three large contributors are 0.47% from the SiN_x ARC surface reflection, 0.46% from the bulk and emitter resistivity and 0.43% from recombination at the local rear Al-contacts. The first one is also plausible since the SiN_x-coated random pyramid surface reflects about 2.4% of the incident photons of a AM1.5G spectrum. Applying the same rule of thumb as for the shadowing above yields 2.4% · 21.2%=

0.50%. The internal bulk & emitter resistance is the largest contributor to the 0.8% power gain due to resistive losses. The contribution of the front Ag-finger grid is considerably smaller because of the 5BB design of the cell. In order to obtain the gain for the bulk & emitter resistance we carry out a simulation of a triple-light-level measurement [16] of a solar cell without front and rear contact resistances and the Ag-finger grid resistance. This results in a measured voltage-dependent lumped series resistance for the bulk and emitter $R_{s,b+em}(V)$. Based on this result and the IV-curve of the basic 21.2%-efficient, we can calculate the enhanced voltages $V_{enh.}$ for an IV-curve of a solar cell without the bulk & emitter resistance: $V_{enh.} = V + R_{s,b+em}(V)\cdot I$. To gain confidence in this result we can support our simulation with some quick analytic calculations. The resistance of the finger grid is R_{grid}=0.17 Ωcm as noted from our SPICE simulation. Using analytic expressions for the resistance of the emitter R_{em} [17], the resistance of the bulk R_b [18] and calculating the contact resistances according to $R_c=\rho_c/f$ with f as the corresponding metallization fractions (4% front side, ~10% rear side) we find R_{grid} = 0.17 Ωcm², R_{em} = 0.15 Ωcm², R_{bulk} = 0.17 Ωcm², $R_{c,front}$ = 0.04 Ωcm², and $R_{c,rear}$ = 0.05 Ωcm². These resistances add up to 0.58 Ωcm, which is close to the total series resistance of 0.62 Ωcm of the 21.2% PERC cell that we measure with the fill factor method. Calculating the relative contribution to the resistance and multiplying with the total resistive power loss will reproduce the results of the simulation with reasonable accuracy, for example $\Delta\eta = (0.17+0.15)/0.62 \cdot 0.8\% = 0.41\%$ for the bulk & emitter contribution. Finally, the recombination at the local Al-contacts with an effective SRV of 300 cm/s is, as expected, the second largest contributor to recombination.

Apart from the single efficiency gains due to deactivation of specific power loss mechanisms Fig. 2 shows two columns for each power loss category (resistance, optics, recombination). The column labeled as “sum” sums up all the individual power gains of the simulations of its category. The columns labeled as “all” in the respective category represent additional simulations that apply simultaneous deactivation of all the power losses of the corresponding category. Comparison of the “sum“ with the “all”-simulation allows the assessment of the impact of nonlinearities or synergies in each category. Simultaneously avoiding all resistive losses leads to an efficiency enhancement of 0.8%, which is equal to the sum. This indicates that all individual resistances add to a total lumped resistance. The sum of all optical gains is 1.6% and thus twice as large as all the resistive gains. A simulation that avoids all the optical losses yields an efficiency gain of 1.7%. There is thus 0.1% synergetic efficiency enhancement due to effects such as the open circuit voltage enhancement due to enhanced photogeneration. Avoiding the various individual recombination losses enhances the efficiency by values that add up to 1.3%. The separate simulation, that applies for the recombination all the ideal values of Table 1 (and thus only contains unavoidable intrinsic bulk recombination), yields 4.3% efficiency increase. The synergetic efficiency enhancement of the recombination losses is thus 3% which makes recombination the most important loss mechanism when compared to optical and resistive efficiency losses. Finally we simulate a cell with all resistive, all optical and all recombination losses replaced by their ideal values. The resulting simulated efficiency is 28.5% and thus 7.3% higher than the efficiency of the experimental 21.2% efficient PERC cell. All individual losses account for 3.7% = 0.8% + 1.6% + 1.3% only. This shows that the synergetic efficiency increase originating from the coupling of the various recombination loss mechanisms is 3.6% and is thus as large as the sum of all individual gains.

The efficiency of our simulated ideal solar cell is still slightly lower than the theoretical limit of 28.8% [19] for a 180 µm thick bulk when considering radiative and Auger recombination as the only loss mechanisms (without photon recycling). This might be due to remaining extrinsic recombination that we allowed in our “ideal” solar cell.

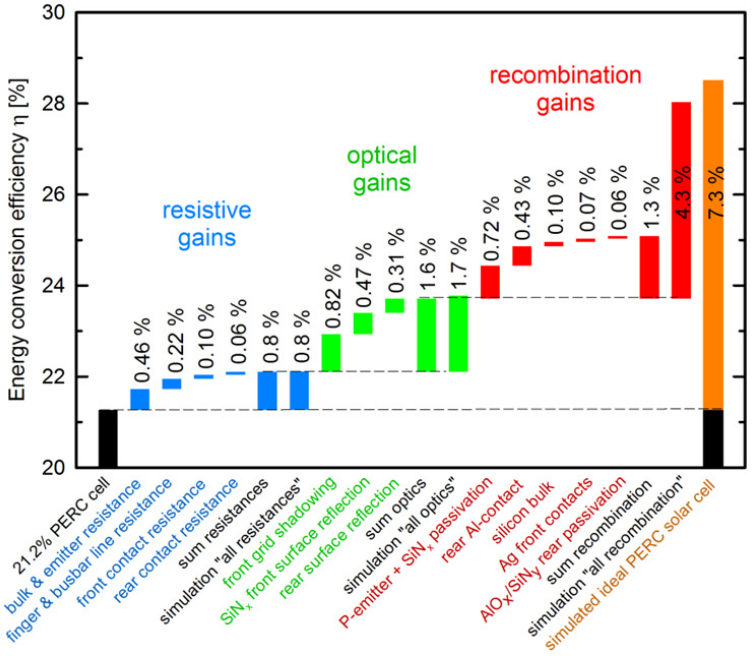

Fig. 2. Absolute gains in efficiency Δη after deactivating single power loss mechanisms. The entries labeled as “sum” sum up the Δη values for a category (i.e. resistance, optics, recombination), whereas the entries labeled as “all” represent simulations with the corresponding parameters set to their ideal values. The “ideal PERC solar cell” models the case that all input parameters assume ideal values.

4. Conclusion

We presented our simulation-based synergetic efficiency gain analysis (SEGA), which allows assessment of the full power gain by improving single power loss mechanisms. Furthermore the SEGA is able to treat resistive, optical and recombinative power losses in an equal manner in terms of their power loss impact. Application of the SEGA to our 21.2%-efficient PERC solar cell shows that synergies of the recombination losses are particularly strong and amount to 3%. They contribute largely to the efficiency gap of 7.3% that our cell has with reference to an ideal cell. The SEGA shows that the power loss due to recombination in the phosphorus-doped emitter and its SiN_x-passivated surface currently limits the solar cell efficiency with a power gain of 0.7%. Another power loss mechanism that allows for large efficiency increases is the shadowing of the finger and busbars with a potential gain of 0.8%, although the cell has a shadowing of only 4% due to its advanced 5BB-design.

References

[1] A. Lachowicz et al., Proceedings 27th European Photovoltaic Solar Energy Conference, Frankfurt, Germany (2012), p. 1846
[2] H. Hannebauer et al., 21.2%-efficient fineline-printed PERC solar cell with 5 busbar front grid, Phys. Status Solidi RRL, (2014), 8: 675–679.
[3] P. J. Verlinden et al., Strategy, development and mass-production of high-efficiency crystalline silicon PV modules, Proc. 6th World Conference on Photovoltaic Energy Conversion (2014), in press
[4] R. Brendel et al., Theory of analyzing free energy losses in solar cells, Appl. Phys. Let. 93(2008), no. 17, 173503
[5] P. J. Verlinden et al., Simple power-loss analysis method for high-efficiency Interdigitated Back Contact (IBC) silicon solar cells, SOLMAT, vol. 106 (2012), pp. 37-41
[6] J. H. Petermann, Ph.D. thesis, University of Hanover, Faculty of Mathematics and Physics, Hanover (2014)
[7] R. Brendel, Sunrays: a versatile raytracing program for the photovoltaic community, Proc. 12th European Photovoltaic Solar Energy Conference (1994), pp. 1339-1342
[8] Sentaurus Process User Guide, Version G-2012.06, Synopsys, Inc., Mountain View, CA, 2012.
[9] Mar. 5, 2015. [Online]. Available: http://www.linear.com/designtools/software/

[10] H. Hannebauer et al., Analysis of the emitter saturation current density of industrial type silver screen-printed contacts, Proc. 27th European Photovoltaic Solar Energy Conference (2012), pp. 1360-1363
[11] C. Kranz et al., Impact of the rear surface roughness on industrial-type PERC solar cells, Proc. 27th European Photovoltaic Solar Energy Conference (2012), pp. 557-560
[12] P. Altermatt et al., Numerical modeling of highly doped Si:P emitters based on Fermi–Dirac statistics and self-consistent material parameters, J. Appl. Phys., 92, 3187-3197 (2002)
[13] L. E. Black et al., Modeling recombination at the Si-Al2O3 interface, Photovoltaics, IEEE Journal of , vol.3, no.3, pp. 936-943, 2013
[14] T. Dullweber et al., Silicon wafer material options for highly efficient p-type PERC solar cells, 39th IEEE Photovoltaic Specialists Conference (2013), pp. 3074-3078
[15] C. Kranz et al., Determination of the contact resistivity of screen-printed Al contacts formed by laser contact opening, Energy Procedia, 2014, in press
[16] K. C. Fong et al., Accurate series resistance measurements of solar cells, Prog. Photovolt: Res. Appl. 2013; 21:490–499
[17] A. Mette, Ph.D. thesis, Albert-Ludwigs-Universität Freiburg im Breisgau, Fakultät für Angewandte Wissenschaften, Freiburg (2007), p. 17
[18] P. Saint-Cast, Ph.D. thesis, University of Konstanz, Department of Physics, Konstanz (2012), pp. 56-61
[19] M. Richter et al., Reassessment of the limiting efficiency for crystalline silicon solar cells, IEEE Journal of Photovoltaics, vol. 3 (2013), pp. 1184-1191